Experimental and Molecular Pathology 111 (2019) 104318

Contents lists available at ScienceDirect

Experimental and Molecular Pathology

journal homepage: www.elsevier.com/locate/yexmp

Ketamine induced cell death can be mediated by voltage dependent calcium channels in PC12 cells

Juanita Bustamante[a,*], Lucas Acosta[a], Analía G. Karadayian[b,c], Silvia Lores-Arnaiz[b,c]

[a] Centro de Altos Estudios en Ciencias Humanas y de la Salud (CAECIHS), Universidad Abierta Interamericana, Montes de Oca 745, 2do piso, 1270AAH Buenos Aires, Argentina

[b] Universidad de Buenos Aires, Facultad de Farmacia y Bioquímica, Cátedra de Fisicoquímica, Buenos Aires, Argentina

[c] CONICET-Universidad de Buenos Aires, Instituto de Bioquímica y Medicina Molecular (IBIMOL), Buenos Aires, Argentina

ARTICLE INFO

Keywords:
Ketamine
VDCC
Cytosolic calcium
Mitochondrial dysfunction
$\Delta\Psi_m$
Cardiolipin
Apoptosis
Necrosis and undifferentiated PC12 cells

ABSTRACT

Ketamine is widely used both as anesthetic and abuse drug. In this study, we investigated the effects of a wide range of ketamine concentrations (100–500–1000 μM) on calcium mobilization and the induction of cell death in undifferentiated PC12 cells, 24 h after treatment. Calcium mobilization was measured as the percentage of fluorescence one minute after depolarization by flow cytometry. For the kinetic changes in $[Ca^{2+}]_c$, fluorescence microscopy with Live Imaging was used with a resolution time of 0.87 s (exposure time: 20 ms). Fluo-4 AM was used for both methods. Flow cytometry using TMRE, NAO, and Annexin V-FITC/PI probes were employed for the evaluation of mitochondrial membrane potential ($\Delta\Psi_m$), cardiolipin content and type of cell death respectively. Fluorescence microscopy was used for the evaluation of DNA fragmentation by TUNEL assay with dUTP-conjugated FITC. Results obtained by flow cytometry showed a clear increment in cell response to depolarization after addition of 50 mM and 70 mM KCl in PC12 cells. Simultaneously, cells treated with 100 μM and 500 μM ketamine during 24 h, induced a decreased response to depolarization as compared with control cells. In addition, 1000 μM ketamine induced a similar increase in Fluo4AM fluorescence either after addition of 50 or 70 mM KCl. The kinetic assays showed that after 100 mM KCl, cells pre-treated with ketamine showed a marked decrease in $[Ca^{2+}]_c$ as compared with control cells. In the case of 1000 μM ketamine treatment, an increased and sustained $[Ca^{2+}]_c$ was observed along the whole assay, indicating a cell disability to maintain calcium homeostasis. Associated with these cytosolic calcium alterations, mitochondrial depolarization, cardiolipin depletion and alteration in Bax protein expression were observed after ketamine treatment. Our data demonstrate that ketamine action in these cells seems to be independent from NMDAR, as observed by the absence of glutamate-calcium response. Acute disturbance in $[Ca^{2+}]_c$ could be mediated by the inhibition of VDCCs as part of the molecular mechanism of ketamine cytotoxicity leading to mitochondrial dysfunction and cell death by apoptosis and necrosis.

1. Introduction

Calcium signals play vital roles in controlling cellular activities through changes in $[Ca^{2+}]_c$ not only in neurons but in many cell types (Cossart et al., 2005), where they function as second messengers and mediate a wide range of cellular responses (Clapham, 2007). The low $[Ca^{2+}]_c$ is maintained by the action of ATP dependent-Ca^{2+} pumps, which pump Ca^{2+} into the two major sinks: the extracellular space and the internal Ca^{2+} stores of the endoplasmic reticulum (ER) and mitochondria (Carafoli and Pedersen, 1987; Clapham, 1995). Increases in $[Ca^{2+}]_c$ can be obtained by the rapid and transient Ca^{2+} influx from the extracellular space to the intracellular medium and by the release from internal stores.

It is known that PC12 cells express L-, N-, and P/Q-type voltage-dependent Ca^{2+} channels (VDCCs) (Dingemans et al., 2009). These VDCCs serve as one of the important mechanisms for Ca^{2+} influx into the cells, enabling the regulation of $[Ca^{2+}]_c$ (Yamakage and Namiki, 2002). The $[Ca^{2+}]_c$ levels play a key role in different signal transduction pathways mediating different biological effects from cell survival to cell death (Choi, 1995; Huang et al., 2013; Sattler and Tymianski, 2001).

It has been observed that cell death can often result from excessive and uncompensated increases in $[Ca^{2+}]_c$. Ketamine can induce toxic effects in cell cultures and animal studies when administered at high

* Corresponding author.
E-mail addresses: Juanita.bustamante@UAI.edu.ar, juanab44@gmail.com (J. Bustamante).

https://doi.org/10.1016/j.yexmp.2019.104318
Received 14 December 2018; Received in revised form 27 September 2019; Accepted 11 October 2019
Available online 12 October 2019
0014-4800/

doses and/or for prolonged periods (Ibla et al., 2009). Cytosolic Ca^{2+} overload has been linked with intracellular events inducing deleterious processes that contribute to neuronal cell death (Huang et al., 2013). Interestingly, different anesthetic agents have been reported to attenuate increases in intracellular calcium concentration, evoked by high potassium in PC-12 cells (Kress et al., 1991). For instance, it has been observed that ketamine inhibits the calcium oscillations in developing hippocampal neurons (Huang et al., 2013). However, the molecular mechanisms induced by the suppression of cytosolic Ca^{2+} signals and their metabolic consequences are still not clearly understood. Thus, both the absence of calcium signals and excessive calcium overload could induce detrimental intracellular consequences associated with cell death. In addition, the source of Ca^{2+} entry appears to be an important factor in the subsequent loss of Ca^{2+} homeostasis and cell death (Ghosh and Greenberg, 1995). Mitochondria contribute to the tight spatio-temporal control of these signals by accumulating Ca^{2+} (Carafoli, 2003), but Ca^{2+} overload leads to subsequent mitochondrial dysfunction (Chen and Chan, 2009). Thus, Ca^{2+} increment beyond the buffering mitochondrial capacity reduces membrane potential and disrupts electron transport chain, leading to increased ROS production (Wang et al., 2010). It is well known that mitochondria are key organelles for cell death induction and regulation through the participation of specific signaling pathways (van Loo et al., 2002).

The differentiated PC12 cell line has been used as a suitable model to study neuronal function and dysfunction (Westerink and Ewing, 2008). We decided to work with undifferentiated PC12 cells due to the fact that these cells not only present an important amount of VDCCs, but also have a lower tendency to form aggregates, and have been used to elucidate different molecular mechanisms related to calcium signaling (Zhu et al., 2019).

Interestingly, cell vulnerability to ketamine treatment could depend on the lineage, its developmental stages, the concentration employed and the time of exposure, influencing different cell death pathways in sensitive cells (Bosnjak et al., 2012). Ketamine concentrations used in our study are toxic, and not related to the anesthetic and antidepressant use of this drug. We previously observed the effect of the exposure of 300 μM ketamine on calcium mobilization in VERO cells (Bustamante et al., 2016). In addition, several studies from other laboratories in different in vitro and in vivo systems used high ketamine concentrations, as described in normal human urothelial cells (Baker et al., 2016), differentiated neurons (Liu et al., 2012) human sperm (He et al., 2016) and rat hippocampus (Demirdaş et al., 2017). Plasma concentrations after anesthetic ketamine doses of 0.250 mg/kg are roughly 180 ng/mL or 1 μM (Clements et al., 1982). As antidepressant, ketamine is most commonly administered in subanesthetic doses of 0.5 mg/kg as an intravenous infusion, for 40 min (Andrade, 2017). The clinically relevant plasma concentrations of ketamine as a non-competitive blocker of N-methyl-D-aspartate receptor (NMDAR) ion channels, which is the known primary mode of action of ketamine, are in line with the IC50 values of ~0.5–1 μM (Glasgow et al., 2017). The ketamine concentrations employed in this study (100, 500, and 1000 μM), although high from a clinical perspective, were selected in order to obtain clear and measurable responses to correlate cytosolic calcium levels with the presence of cell death pathways via apoptosis and necrosis (Wang et al., 2017). In addition, despite the reported resurgence of ketamine abuse, limited literature is available on the ketamine concentrations attributed to toxic doses (Lalonde and Wallage, 2004). Then, the observed high levels of ketamine consumption during abuse conditions (Wood et al., 2011) could also justify the use of the high concentrations in the present study. Since changes in $[Ca^{2+}]_c$ are highly dynamic and constitute important readouts in neurotoxicological and neuropharmacological studies, we employed fluorescence microscopy with Live Imaging with a resolution time of 0.87 s, allowing us to detect real time calcium response to depolarization after ketamine treatment.

The aim of this work was to analyze alterations in $[Ca^{2+}]_c$, mitochondrial function and induction of cell death after exposure of undifferentiated PC12 cells to a wide range of ketamine concentrations.

2. Materials and methods

2.1. Materials

DMEM, fetal bovine serum (FBS) and horse serum were from Gibco BRL (Gaithersburg, MD, USA). Fluo-4 acetoxymethyl (Fluo-4 AM), tetramethyl-rhodamine-ethyl ester (TMRE) and 10 N-nonylacridine orange (NAO) were obtained from Invitrogen Corporation (Invitrogen, USA). Poly-L-lysine, ionomycin, Annexin-V and propidium iodide were purchased from Molecular Probes. (±)-Ketamine hydrochloride was from Novartis Argentina S.A. TUNEL Label Mix and TUNEL enzyme were from ROCHE. Carbonyl cyanide4-(trifluoromethoxy)-phenylhydrazone (FCCP), etoposide and all the other drugs were from SIGMA.

2.2. Cell culture and ketamine treatment

Undifferentiated PC12 cell line was obtained from the American Type Culture Collection (ATCC), grown in DMEM supplemented with 10% FBS, 5% horse serum, 2 mM glutamine, 50 U/mL penicillin and 50 μg/mL streptomycin. Cells were cultured in T25 bottles, 6-well plates and coverslips previously coated with 5% poly-L-lysine, and incubated as previously described (Bustamante et al., 2016). For calcium measurement cells were cultured in hand-made glass-bottom dishes (dos Santos Claro et al., 2019) and used directly with no trypsinization. After semiconfluency, cells were exposed for 24 h to a wide range of (±)-Ketamine-hydrochloride concentrations -100μM, 500 μM, 1000 μM- and untreated cells being exposed only to saline buffer. Prior to use, cells were washed two times with Hepes–buffered saline solution (HBSS) consisting in mM: 116 NaCl, 5.4 KCl, 0.8 $MgSO_4$, 1.3 NaH_2PO_4, 12 HEPES, 5.5 glucose, 25 bicarbonate solution at pH 7.45.

2.3. Cell response to depolarization was analyzed by flow cytometry with Fluo-4 AM

Flow cytometry was performed in a FACScalibur (Becton-Dickinson) equipped with a 488 nm argon laser and a 615 nm red diode laser. Cells (1×10^6) were collected and suspended in 1 mL HBSS loaded with 250 nM Fluo-4 AM for 30 min at 37 °C in the dark. After loading, cells were washed again and suspended in 1 mL of HBSS, plus 1 mM $CaCl_2$. After measuring basal fluorescence, cell suspension was exposed to different levels of depolarization, which were induced with a fixed volume of different stock solutions of KCl to obtain final concentrations of 50 and 70 mM, and the fluorescence intensities obtained after 1 min were recorded (Wong and Martin, 1993). The percentage of fluorescence (FL-1) intensity histograms, under the marker M1 (events with high r.f.i.) was analyzed and quantified. As controls of maximum and minimal fluorescence intensity, experiments were performed with cells exposed to 10 μM ionomycin and 10 mM EDTA plus 10 mM EGTA respectively. Data were expressed as mean % ± SEM.

2.4. Fluorescent microscopy Ca^{2+} imaging in ketamine treated undifferentiated PC12 cells

Cells were subcultured (200×10^3) in poly-L-lysine (50 μg/mL) coated hand-made glass-bottom dishes at 60% confluence. Next, cells were loaded with Fluo-4 AM during 30 min at 37 °C and placed on the stage of an Axiovert 35 M inverted microscope with Live Imaging system (40× oil-immersion objective, NA 1.0: Zeiss, Gottingen, Germany) equipped with a TILLPhotonics Polychrome IV (Xenon Short Arc lamp, 150 W; TILL Photonics GmBH, Gräfelfing, Germany). Fluo-4 AM fluorescence was evoked at 488 nm and collected at 520 nm, every 0.87 s (exposure: 20 ms), with an Image SensiCam digital camera (TILL Photonics GmBH, Gräfelfing, Germany). No significant dye bleaching occurred in these assays. Experiments were performed at

37 °C and consisted of a 40 s baseline recording and a 1.5 min subsequent depolarization, by 100 mM KCl in order to obtain an adequate response. To assess dynamic ranges for microscopy, maximum and minimum fluorescence values were determined in separate experiments in which Fluo-4 AM loaded PC12 cells were incubated with ionomycin (5 μM) and ethylenediamine-tetraacetic acid (EDTA: 10 mM) respectively. Cell fluorescence values were converted to absolute $[Ca^{2+}]_c$ according to the equation $[Ca^{2+}]_c = Kd\ [F - F_{min}]/[F_{max} - F]$, where Kd for Fluo-4 AM = 345 nM. Calcium-imaging data were analyzed using a digital imaging software (FIJI, ImageJ 1.52n). Three independent experiments were performed and values of fluorescence from 30 cells (n) were converted to absolute $[Ca^{2+}]_c$ as described above. Data were expressed as mean ± SEM of absolute calcium concentrations in nM, for each condition.

2.5. Analysis of mitochondrial membrane potential by flow cytometry

The mitochondrial transmembrane potential ($\Delta\Psi_m$) contributes mostly to the proton motive force, validating its determinations in intact cells after loading with the potentiometric fluorescent lipophilic cation TMRE. Cells (1×10^6) after ketamine treatment (100 μM, 500 μM and 1000 μM), were suspended in 1 mL of HBSS, followed by 40 min incubation with TMRE at 37 °C (Bustamante et al., 2004), and immediately acquired by the cytometer. Fluorescence changes were collected through FL-2 histograms (not shown) using 5 μM FCCP as positive control. FCCP is an uncoupler of oxidative phosphorylation indicating maximal mitochondrial depolarization. Three different experiments were performed and results were expressed as mean ± SEM.

2.6. Analysis of mitochondrial cardiolipin content by flow cytometry

The fluorophore NAO binds tightly to the acidic phospholipid cardiolipin, localized exclusively in internal mitochondrial membranes and can be used to quantify mitochondrial cardiolipin content (Petit et al., 1994). After ketamine treatment, cells were suspended in 1 mL HBSS, loaded with 100 nM NAO during 40 min at 37 °C in the dark and immediately acquired by the cytometer. Fluorescence response was analyzed by fluorescence histograms of the different samples (not shown). Three different experiments were performed and results expressed as mean ± SEM as shown in a bar graph.

2.7. Western blot analysis of mitochondrial BAX protein expression

Cells (1×10^6) were lysed and equal protein amounts (80 μg) of the mitochondrial pellet were loaded onto a 12% SDS-PAGE and transferred to a nitrocellulose membrane (Millipore, Atlanta, GA, USA). Non-specific binding was blocked with 5% defatted milk powder, followed by immunoblotting with a dilution 1:500 of polyclonal primary antibodies specific for Bax at 4 °C overnight, then incubated with HRP-conjugated secondary antibodies at room temperature for 1 h. Following each step, the membranes were washed with PBS for 3 min. Chemiluminescence (ECL) system (Pierce) was used. Densitometry was performed using ImageJ 1.47 v and the expression of Bax was determined by calculating the gray scale value ratio to β-tubulin band to normalize data. The ratio of Bax/β-tubulin was estimated for each cell condition. Three different experiments were performed, and results were expressed as mean ± SEM.

2.8. Cell death analysis by DNA fragmentation: TUNEL assay

Cell DNA fragmentation after ketamine treatment was analyzed using the terminal deoxynucleotidyl transferase dUTP nick-end labeling (TUNEL) assay (Darzynkiewicz et al., 2008). Briefly, cells harvested as described before were seeded in a microscope slide during 20 min, and prefixed with 300 μL of 3.7% formaldehyde in PBS during an additional period of 20 min at 4 °C. Then cells were washed, permeabilized with 300 μL of 70% ethanol during 10 min at 4 °C and washed again with PBS. Slides were covered with 100 μL of the reaction mixture (10 μL of 10× TDT buffer, 30 μL of H_2O, 5 μL of TUNEL enzyme and 50 μL of TUNEL Label Mix, containing dUTP-conjugated with FITC) and incubated for 40 min at 37 °C in the dark. A negative control was included, processed identically but without the enzyme (TdT) (not shown). Etoposide (1 μM) was used as a positive apoptotic control. Slides were mounted and analyzed by epifluorescence microscope (Arcano XSZ 107 BNT YX) equipped with a camera (MOTICAM1000). A xenon lamp was used for excitation at 488 nm and emission wavelength at 525 nm. Quantification of the TUNEL assay was performed by counting positive fluorescent cells after evaluation of 100 micrographs for each sample in 3 different experiments and expressed as % of untreated control cells (% mean ± SEM).

2.9. Apoptosis and necroptosis analysis by phosphatidyl-serine exposure: double binding of PI/Annexin V-FITC

Flow cytometry allows simultaneous multiparametric analysis for dying cells measurement. Annexin V was used to detect phosphatidyl-serine (PS) externalization (Chris et al., 1995; Reutelingspergerg, 1990; Tait et al., 1989) and the level of DNA fragmentation was quantified by Propidium iodide (PI) staining. After treatment with the different ketamine concentrations, and etoposide as positive apoptotic control, cells were harvested, suspended in 500 μL of binding buffer plus 3 μg/mL Annexin V-FITC and incubated during 30 min at room temperature in the dark. After staining with 20 μL of 30 mM PI solution during additional 10 min, cells were immediately acquired by flow cytometry. Single-PI and single-Annexin V-FITC stained controls for compensation assays were performed. FACS analysis of cells undergoing necroptosis was performed by gating a specific cell population. Graphic representation of the cell fluorescence response PI/Annexin V-FITC is shown in a typical dotplot. Quantification of the type of cell death was shown by a bar-graph representation as % of PI/Annexin positive cells. Results were expressed as the mean ± SEM of three independent experiments.

2.10. Statistical analysis

All experiments were repeated three times, and results are presented as mean ± SEM. Prior to each flow cytometry analysis, test variables were checked for normality by the Kolmogorov-Smirnov test. ANOVA followed by Tukey's test was used to analyze differences between mean values of more than two groups. SPSS (13.0 version) statistical software was used and a difference was statistically significant when $p < .05$.

3. Results

3.1. Cell response to different levels of KCl depolarization

The fluorescence response of untreated, ketamine treated during 24 h, EDTA + EGTA and ionomycin exposed cells, was performed after 1 min of KCl-induced depolarization. Typical Fluo-4 AM fluorescent histograms after 70 mM KCl are shown in Fig. 1a. Cells exposed to increased levels of depolarization with 50 mM and 70 mM KCl, showed an increase in the percentage of fluorescence intensity in control, 100 and 500 μM ketamine treated cells, being 56%, 41% and 37% respectively as observed in Fig. 1b. Meanwhile, cell treated with 1000 μM ketamine induced only an increment of 25%. Interestingly, undifferentiated PC12 cells stimulated with 250 mM glutamate (Wong and Martin, 1993) did not show increments in fluorescence (Fig. 1b).

3.2. Cytosolic Ca^{2+} measurement by fluorescence microscopy

The effects of 24 h-ketamine treatment on calcium influx in PC 12 cells after 100 mM KCl-induced depolarization are described in Fig. 2a.

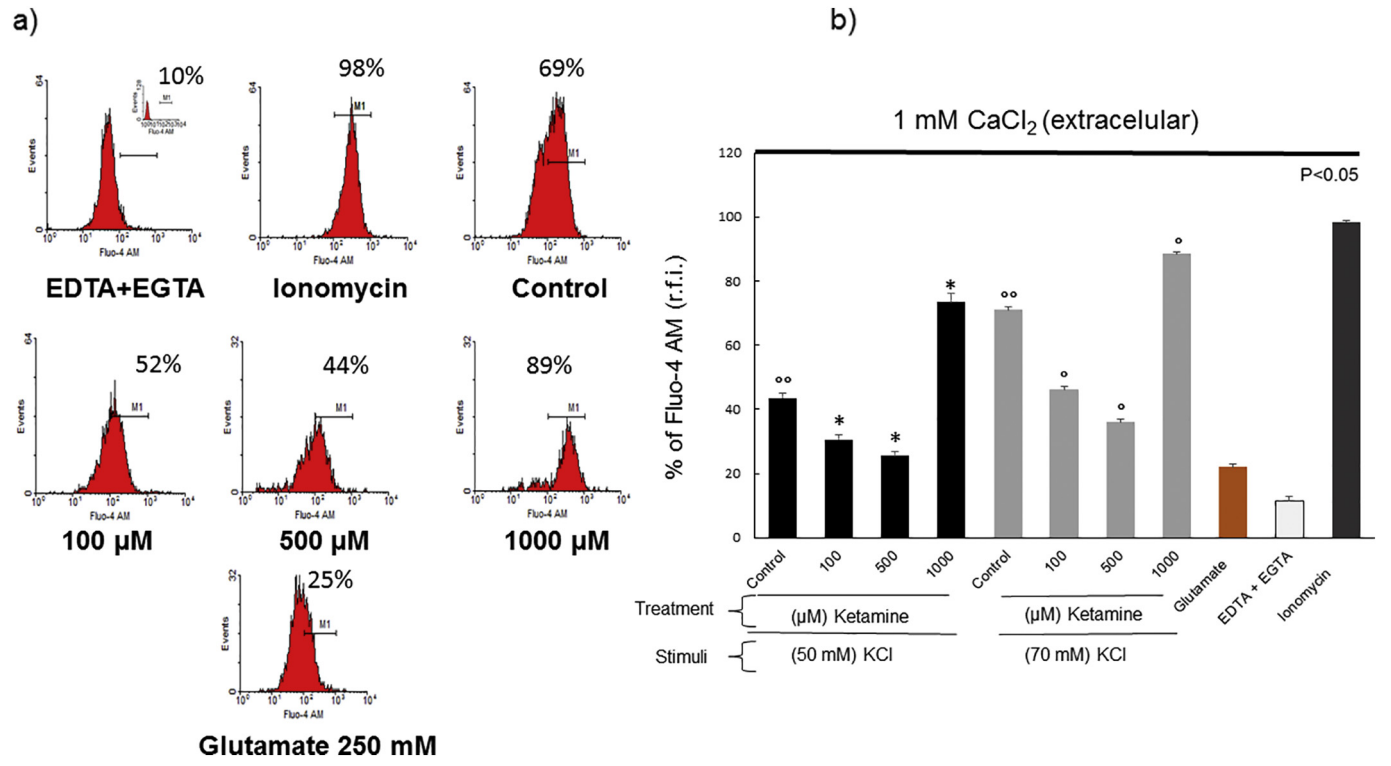

Fig. 1. Undifferentiated PC12 response to different levels of depolarization.
Cells after 100, 500, and 1000 µM ketamine treatment for 24 h, were collected, loaded during 30 min with Fluo-4 AM and acquired by the cytometer for basal measurements. After 1 min of exposure to 50 and 70 mM KCl, cells were acquired again for fluorescence (FL-1) analysis. 1a) Typical flow cytometry assay with fluorescence histogram for controls and treated cells after 70 mM KCl is shown. 1b) Quantification of (r.f.i.) after 50 mM and 70 mM KCl, and 250 mM glutamate for control and ketamine treated PC12 cells is shown as a bar graph, data were expressed as mean % ± SEM from three different experiments. Ionomycin and EDTA were used as controls.

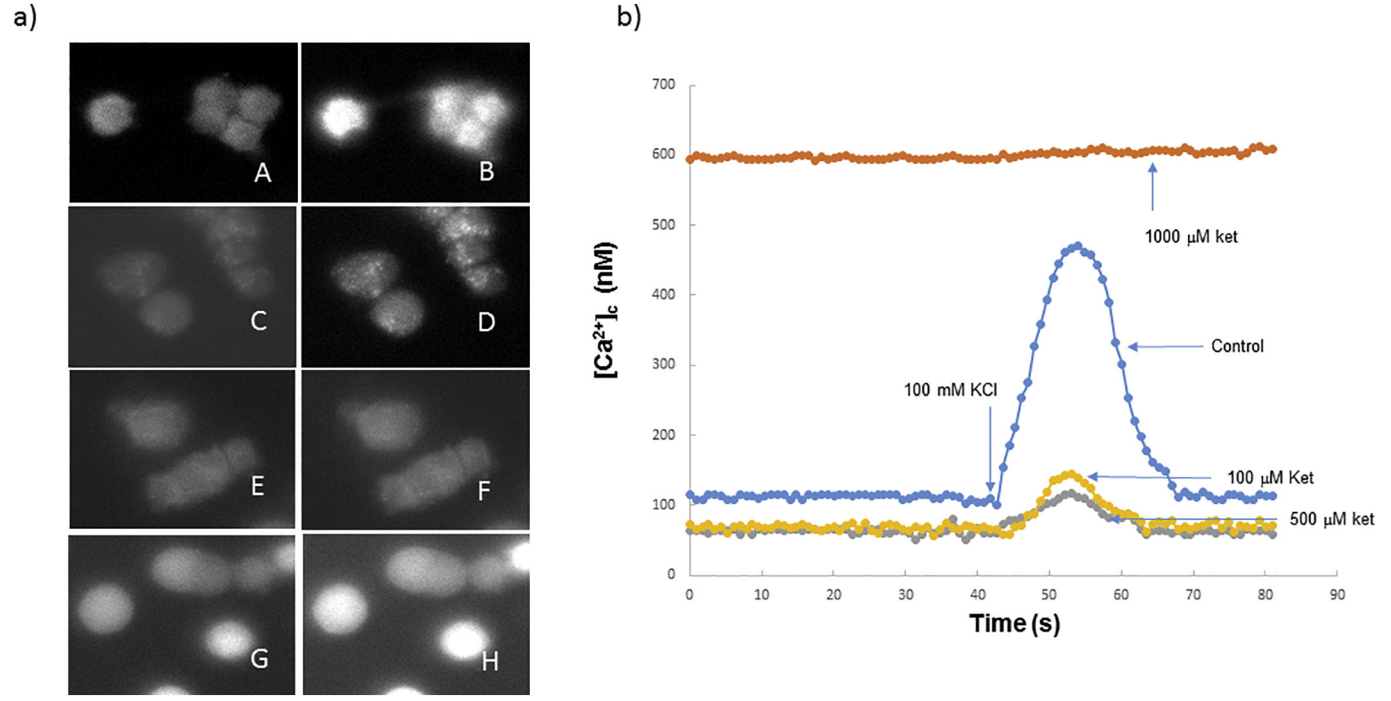

Fig. 2. Epifluorescence microscopy with live imaging was used to record the kinetics of cell calcium mobilization in undifferentiated PC12 cells.
Cells were exposed to 100 µM, 500 µM and 1000 µM ketamine for 24 h. Calcium mobilization from the extracellular buffer to the cytoplasm were scanned in a fluorescence microscope after 100 mM KCl stimulated Fluo-4 AM loaded cells. 2a. Cell images before and after 40 s of 100 mM KCl exposure for control A) and B); 100 µM ketamine C) and D); 500 µM ketamine E) and F); and 1000 µM ketamine treated cells G) and H) are shown. 2b, graph with traces illustrating the changes in $[Ca^{2+}]_c$, during 30 s before and after KCl depolarization, with a resolution time of 0.87 s.

Calcium images before depolarization showed low levels of intracellular calcium in control cells as well as after 100 μM and 500 μM treatment with ketamine (A, C, E). After depolarization, the fluorescence intensity increased clearly in untreated cells (B), meanwhile only a slight increase was observed in 100 μM (D) and 500 μM (F) ketamine treated cells. Cells treated with 1000 μM ketamine showed an increased fluorescence intensity before depolarization (G) that was preserved after KCl addition (H). As shown in Fig. 2b. after 100 mM KCl-induced calcium influx, the amounts of intracellular calcium increased time-dependently in control cells, showing intracellular calcium transients, from 112 ± 4 nM up to 460 ± 3 nM, while cells incubation with 100 μM and 500 μM ketamine induced a very slight increase in cytosolic calcium transients, from 66 ± 2 up to 118 ± 6 nM and 65 ± 3 up to 143 ± 4 nM respectively. This results indicate strong cytosolic calcium decreases of 85% and 78% respectively as compared with untreated cells. Meanwhile, cell treatment with 1000 μM ketamine showed an increased cytosolic calcium level (594 ± 2 nM) before depolarization, which was sustained after KCl addition (605 ± 12 nM).

3.3. Ketamine effect on mitochondrial membrane depolarization

Changes in $\Delta\Psi_m$ after ketamine exposure during 24 h were described in Fig. 3a. Mitochondrial depolarization was quantified after 100 μM, 500 μM and 1000 μM ketamine cells treatment, showing increases in mitochondrial depolarization of 24%, 27% and 52% respectively, as compared with untreated cells. As expected, the positive controls with FCCP and etoposide showed 38% and 41% increases of mitochondrial depolarization as compared with the untreated cells.

3.4. Ketamine effect on mitochondrial cardiolipin content

Decrease in NAO fluorescence could be related to a decrease in the mitochondrial cardiolipin content due to cardiolipin peroxidation/depletion. Fig. 3b shows the quantification of the fluorescence cell response in a bar graph for each cell condition after 24 h treatment. Cardiolipin content did not change after cells incubation with 100 μM ketamine and only a 7% decrease was observed after 500 μM ketamine cells treatment. On the contrary, significant cardiolipin depletion of 32% was observed after cells treatment with 1000 μM ketamine.

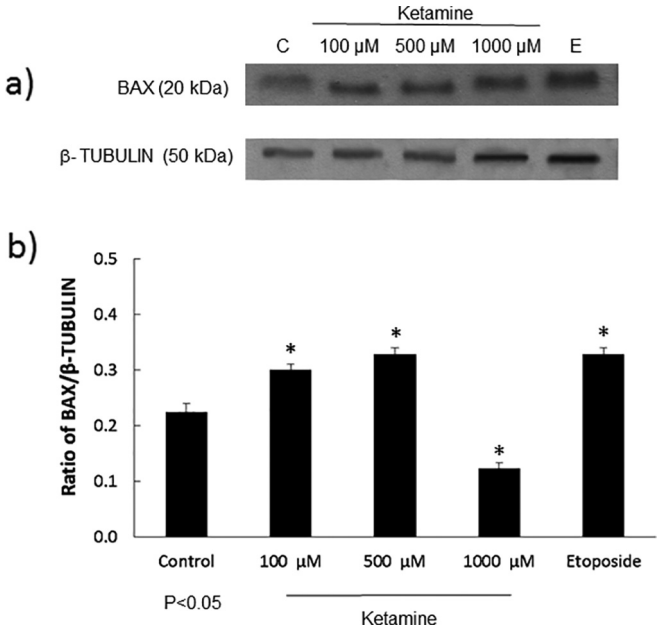

Fig. 4. a and b. Bax protein expression. After ketamine treatment mitochondrial Bax/β-tubulin ratio was determined by Western blot. a) Inmunoblots from a representative experiment. b) Bar graph describe the Bax/β-tubulin ratio (mean ± SEM) after three different experiments. (*p < .05).as compared with untreated cells.

Cardiolipin depletion of 49% was also detected after etoposide treatment as compared with untreated cells. These results indicate that cells treatment with 1000 μM ketamine, induced a high mitochondrial cardiolipin peroxidation.

3.5. Ketamine effect on Bax protein expression

Bax association to the outer mitochondrial membrane was analyzed by Western blot after ketamine treatments during 24 h, as shown in Fig. 4. The results showed an increased band of 20 kDa in cells treated with 100 μM and 500 μM ketamine, and etoposide treatments as

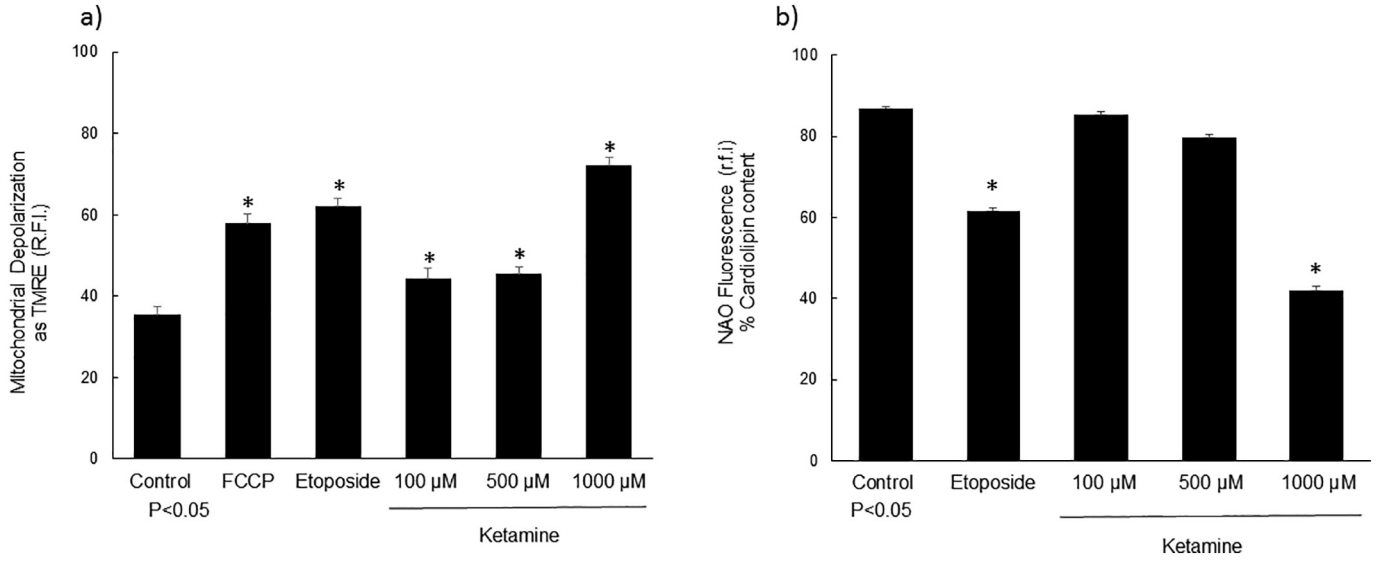

Fig. 3. a and b. Effect of ketamine on mitochondrial depolarization and cardiolipin content. a) Cells were treated for 24 h with 100, 500, and 1000 μM ketamine, harvested and loaded with TMRE. FCCP and etoposide were used as depolarizing and apoptotic controls. Quantification of the ΔΨm loss was described in the bar graph, significant differences for 100, 500 and 1000 μM ketamine treatment were observed as compared with untreated cells (*p < .05), b) After ketamine treatment for 24 h, cells were harvested and loaded with NAO. Quantification of cardiolipin oxidation/depletion is described in the bar graph, etoposide was used as apoptotic control. Differences were compared with untreated (control) cells (*p < .05).

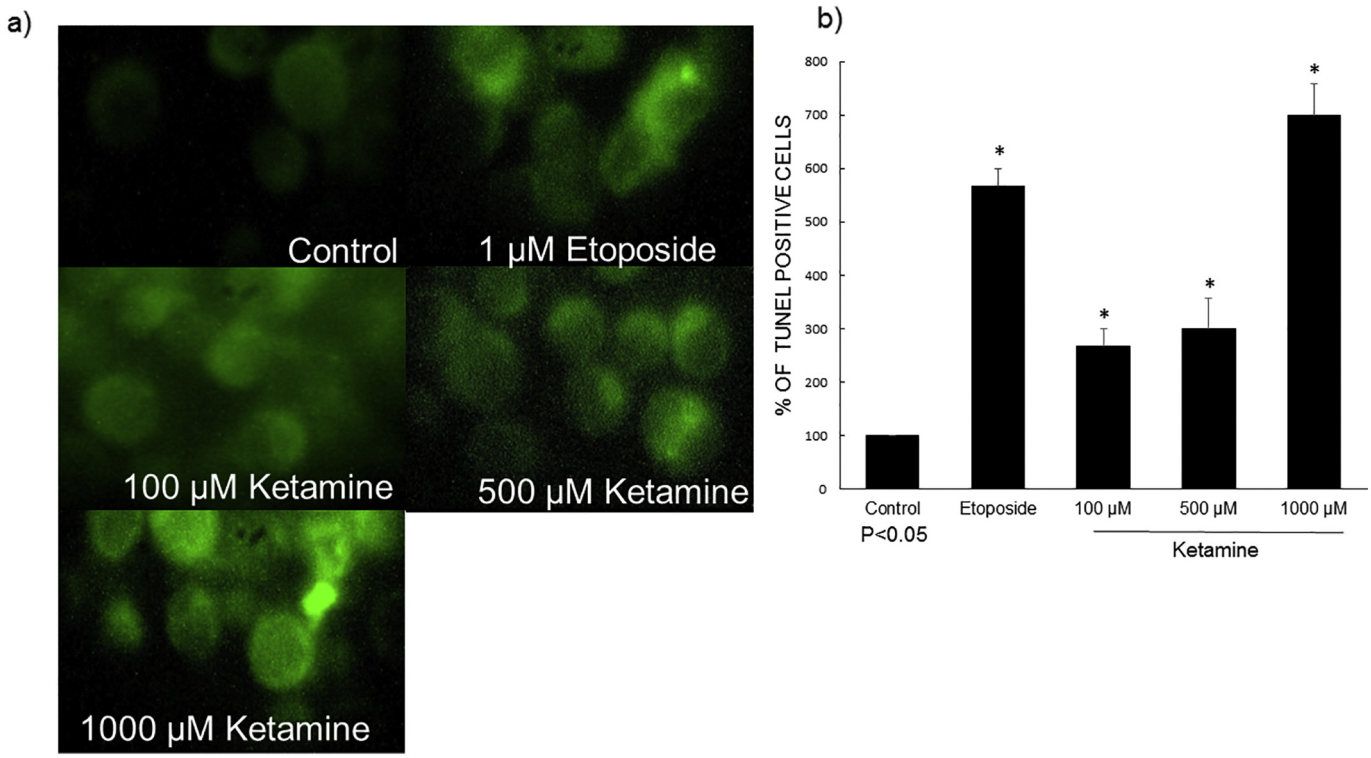

Fig. 5. a and b. DNA fragmentation by TUNEL assay in PC12 cells. Cells were treated for 24 h with 100, 500, and 1000 μM ketamine. a) Epifluorescence cell images (100×) after ketamine treatment. b) Quantification of TUNEL positive cells. (*p < .05) as compared with the control values.

compared with untreated cells. The bar-graph of Bax/β-tubulin ratio for 100 and 500 μM ketamine and etoposide treatments showed increments of 34%, 46% and 46% respectively as compared with untreated samples. Interesting but not clearly understood was the fact that cells treated with 1000 μM ketamine presented 45% decrease in the Bax/β-tubulin ratio, showing all of them significant differences of Bax/β-tubulin ratio as compared with untreated-control samples.

3.6. Analysis of PC12 cell death after treatment with different ketamine concentrations

3.6.1. TUNEL results

Fluorescence microscopy evaluated the level of DNA fragmentation by dUTP-FITC after ketamine treatment during 24 h, as shown in Fig. 5a. Quantification of these results as the percentage of untreated-control cells showed 227% and 300% of TUNEL positive cells after 100 μM and 500 μM ketamine treatment respectively. Treatment with 1000 μM ketamine showed the highest number of TUNEL positive cells, being 700% (Fig. 5b) meanwhile Etoposide used as a positive control showed 567%. This difference could be due to the fact that in the case of cells treated with 1000 μM ketamine apoptosis and necrosis were occurring simultaneously.

3.6.2. Type of cell death

The type of cell death was determined by cytometry with Annexin V-FITC/PI binding (Crowley et al., 2016). A typical experiment of double binding is shown in Fig. 6a. Annexin V can also be used to detect necrosis, due to the fact that necroptotic cells become Annexin V-positive. However, when combined with PI, the double-labeling procedure allows a further distinction of necrotic (Annexin V+/PI+) from early apoptotic (Annexin V+/PI−) cells. Quantification of apoptotic, necroptotic and viable cells was described after ketamine treatment during 24 h as a bar graph in Fig. 6b. The amount of PS externalization, occurring in early apoptotic cells was 2% and 34% for untreated and etoposide treated cells respectively. Meanwhile, after ketamine treatment with 100 μM and 500 μM, cells showed apoptotic levels of 17% and 12% respectively. A high apoptotic level was observed after 1000 μM ketamine treatment being 35%, similar to the etoposide positive control. Low levels of necrotic cells were observed both in untreated and in apoptotic control samples, being 4% and 8% respectively. Similar necroptosis levels were observed after 100 μM and 500 μM ketamine treatment, being 5% and 9%, while after 1000 μM ketamine treatment the presence of necroptosis increased to 22%. Whereas living or viable cells (91%) in untreated cells remained Annexin-V-negative, a clear decrease was observed after cells treatment with ketamine 100 μM and 500 μM, being 75% and 79% respectively. Only 45% viable cells were observed after 1000 μM ketamine treatment, being similar to the percentage of living cells in the apoptotic control (55%).

4. Discussion

In neuronal cells, Ca^{2+} plays an essential role in a large number of cellular processes, including neurotransmission, gene expression and programmed cell death (apoptosis), as well as necrotic cell death (Zhivotovsky and Orrenius, 2011), via mitochondrial disruption and release of degradative enzymes. In neuronal cells, a strong control over their Ca^{2+} signals is exerted, tightly regulating the balance between Ca^{2+} influx, extrusion, sequestration and buffering by cytosolic Ca^{2+} binding proteins (Westerink and Ewing, 2008). As a result, Ca^{2+} signals are highly dynamic with rapid and transient, increases and oscillations that occur in seconds to minutes (Eilers et al., 1995). It is important to highlight that PC12 cell cultures present important advantages in studies of the molecular mechanisms related to drug action, although they showed important limitations of data extrapolation to the clinical human therapy.

The results of the present study showed an increased calcium cell response to depolarization, 1 min after cell exposure to different concentrations of KCl. This increased cytosolic calcium measured as Fluo-4 AM fluorescence seems to be mediated by the opening of VDCC, L-

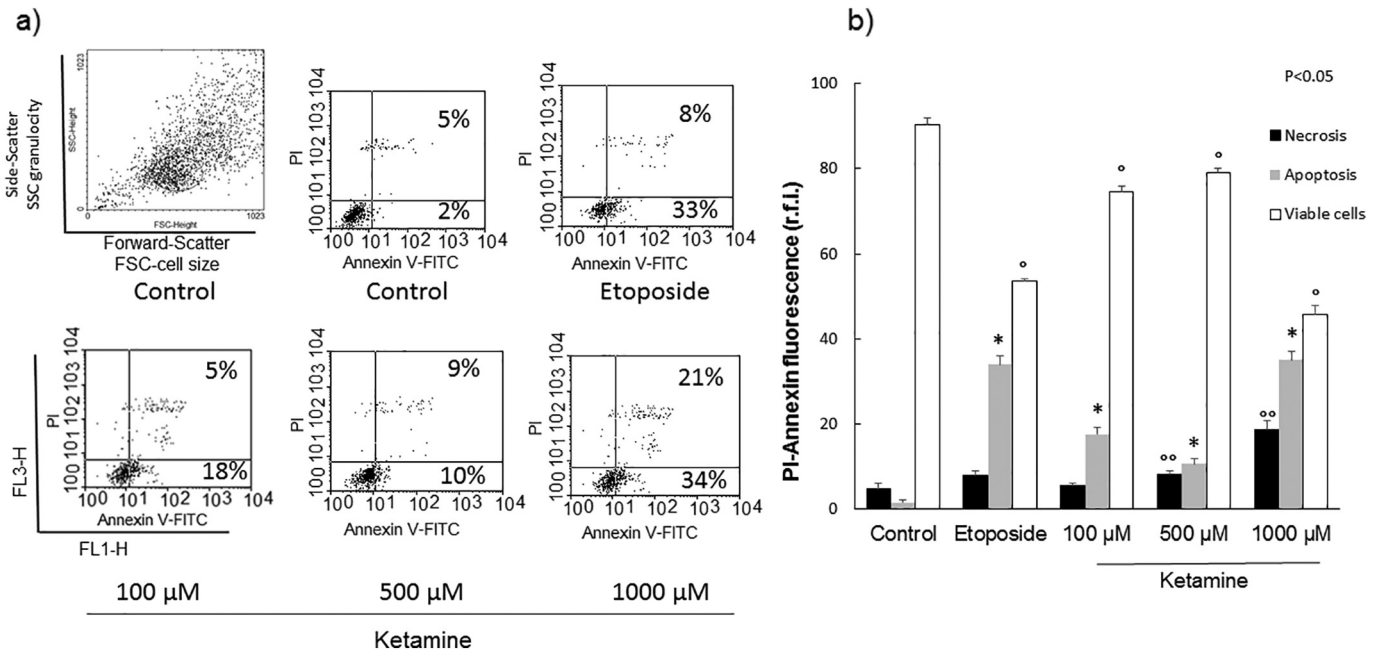

Fig. 6. a and b. Flow cytometry analysis of cell death by double binding of Annexin V-FITC and propidium iodide. Cells were treated for 24 h with 100, 500, and 1000 µM ketamine. a) Typical dotplot quadrant of double binding with PI/Annexin-V is shown in Fig. 6a, allowing to detect the percentage of cell death types in each PC12 condition. The double-labeling procedure allows a further distinction between necrotic (Annexin V+/PI+) and early apoptotic (Annexin V+/PI−) cells. Etoposide was used as a control of apoptotic cell death. b) Quantification of viable, apoptotic induced and necroptotic cells was described as a bar graph for each PC12 condition. The results indicate significant differences for cell viability, apoptosis and necrosis after etoposide, 100, 500 and 1000 µM ketamine treatments (*$p < .05$) as compared with untreated cells.

and N-type, present in PC12 cells (Avidor et al., 1994) as a result of KCl-induced depolarization. The absence in Ca^{2+}-response of PC12 cells to glutamate, suggests that the inhibitory effect of ketamine on cytosolic Ca^{2+} transport does not seem to be mediated by NMDAR.

In this study, intracellular calcium dynamics in ketamine treated undifferentiated PC12 cells was studied by real-time kinetic measurements of Ca^{2+} using fluorescence microscopy assays. The kinetic studies of $[Ca^{2+}]_c$ performed by fluorescence microscopy with the highest level of depolarization provide clear evidence that ketamine at concentrations of 100 µM and 500 µM presented decreased intracellular calcium transients as compared with untreated cells. This observation suggests that the inhibition of depolarization-evoked Ca^{2+}-influx could be mediated by VGCCs in agreement with Wong and Martin, 1993. The simultaneous lack of depolarization response and high $[Ca^{2+}]_c$ observed after 1000 µM ketamine treatment could be also due to an equilibrium between extra and intracellular calcium in dying cells were the death program has already begun.

The interesting point of this study is the evidence that all the ketamine doses employed were able to induce apoptotic processes although with different intensity as indicated by the simultaneously performed TUNEL and early PS externalization assays. The cell death signaling to necrosis was important only at high ketamine concentrations. Increased $[Ca^{2+}]_c$ has been associated with different models of apoptosis (Nicotera and Orrenius, 1998) which induce Ca^{2+} signals produced by influx from the extracellular space or by mobilization from intracellular stores (Nicotera and Orrenius, 1998; Krieger and Duchen, 2002).

In this study, the observed cell death signaling included mitochondrial mediation showing cardiolipin depletion and decreased $\Delta\Psi_m$. It is known that alterations in calcium homeostasis have deleterious consequences for mitochondria. In fact, mitochondrial calcium retention capacity is reduced in different conditions inducing a loss of the mitochondrial transmembrane potential (Carafoli, 2003). In previous studies we observed a clear inhibition of the ability of mitochondria from ketamine injected animals to accumulate Ca^{2+}, as compared with mitochondria from saline injected rats (Bustamante et al., 2016). Mitochondrial cardiolipin depletion observed after ketamine treatment could be related to the fact that the presence of this phospholipid at the inner mitochondrial membrane and its proximity with the mitochondrial sites of reactive oxygen species production, make this molecule an important target for peroxidative processes (McMillin and Dowhan, 2002). Cardiolipin alterations would induce a dysfunction in the respiratory mechanism and therefore could risk the ATP output to match cellular energetic demand.

In addition, the important level of mitochondrial depolarization after ketamine treatment could be related in part to the presence of the Bax protein in mitochondrial outer membrane changing the ratio between pro- and antiapoptotic members and consequently leading to apoptotic processes. It is well known that the mitochondrial protein membrane ratio of the Bcl-2 family members can contribute not only to control different mitochondrial pathways of apoptosis but also to alter cytosolic Ca^{2+} homeostasis and mitochondrial energetics (D'Orsi et al., 2017; Nutt et al., 2002; Scorrano et al., 2003). The low mitochondrial Bax/β-tubulin ratio observed at high ketamine concentrations, could be related with an increased protein degradation as the result of the observed necrotic process.

In this study toxic concentrations of ketamine were able to induce a disruption in PC12 cells calcium transport machinery, probably mediated by alterations in calcium mobilization through VDCC, eliciting different signaling cascades that would change cell fate, and induce mitochondrial dysfunction and cell death by apoptosis and necrosis.

5. Conclusions

Current data demonstrate that PC12 cells after treatment with ketamine concentrations responded to different levels of KCl-depolarization being also able to inhibit K^+-induced calcium increase probably by inhibition of VDCCs. Meanwhile, after treatment with high concentrations of ketamine, a low response to depolarization, and a disability to manage calcium was evident. The results also showed that the

alterations in $[Ca^{2+}]_c$ could result in adverse cellular effects, leading to cell death by apoptosis mediated by mitochondrial dysfunction. In the case of cell exposure to high concentration of ketamine, the increased $[Ca^{2+}]_c$ was associated with an increased level of apoptosis and necrosis.

Declaration of Competing Interest

The authors state that there are no conflicts of interest pertaining to this manuscript.

Acknowledgments

The authors wish to thank Dr. Sandra Verstraeten for her help with PC12 cell line. This research was supported by grants from Centro de Altos Estudios en Ciencias Humanas y de la Salud (CAECIHS, PS1/CAE 2017), Universidad Abierta Interamericana, Buenos Aires, Argentina. Consejo Nacional de Investigaciones Científicas y Técnicas (CONICET, PIP 112-20150100648), and Universidad de Buenos Aires (UBA, 0020130100255BA), Argentina.

References

Andrade, C., 2017. Ketamine for depression, 1: clinical summary of issues related to efficacy, adverse effects, and mechanism of action. J. Clin. Psychiatry 78, e415–e419. https://doi.org/10.4088/JCP.17f11567.

Avidor, B., Avidor, T., Schwartz, L., De Jongh, K.S., Atlas, D., 1994. Cardiac L-type Ca^{2+} channel triggers transmitter release in PC12 cells. FEBS Lett. 342, 209–213.

Baker, S.C., Shabir, S., Georgopoulos, N.T., Southgate, J., 2016. Ketamine-induced apoptosis in normal human urothelial cells: a direct, N-methyl-D-aspartate receptor-independent pathway characterized by mitochondrial stress. Am. J. Pathol. 186, 1267–1277. https://doi.org/10.1016/j.ajpath.2015.12.014.

Bosnjak, Z., Yan, Y., Canfield, S., Muravyeva, M., 2012. Ketamine induces toxicity in human neurons differentiated from embryonic stem cells via mitochondrial apoptosis pathway. Curr. Drug Saf. 7, 106–119. https://doi.org/10.2174/157488612802715663.

Bustamante, J., Di Libero, E., Fernandez-Cobo, M., Monti, N., Cadenas, E., Boveris, A., 2004. Kinetic analysis of thapsigargin-induced thymocyte apoptosis. Free Radic. Biol. Med. 37, 1490–1498. https://doi.org/10.1016/j.freeradbiomed.2004.06.038.

Bustamante, J., Czerniczyniec, A., Lores-Arnaiz, S., 2016. Ketamine effect on intracellular and mitochondrial calcium mobilization. Biocell 40, 11–14.

Carafoli, E., 2003. Historical review: mitochondria and calcium: ups and downs of an unusual relationship. Trends Biochem. Sci. 28, 175–181. https://doi.org/10.1016/S0968-0004(03)00053-7.

Carafoli, E., Pedersen, P., 1987. Ion motive ATPases. Ubiquity, properties, and significance to cell function. Ann. N. Y. Acad. Sci. 146–151. https://doi.org/10.1111/j.1749-6632.1998.tb11202.x.

Chen, H., Chan, D.C., 2009. Mitochondrial dynamics-fusion, fission, movement, and mitophagy-in neurodegenerative diseases. Hum. Mol. Genet. 18, 169–176. https://doi.org/10.1093/hmg/ddp326.

Choi, D.W., 1995. Calcium: still center-stage in hypoxic-ischemic neuronal death. Trends Neurosci. 18, 58–60. https://doi.org/10.1016/0166-2236(95)80018-W.

Chris, R., Vermes, I., Haanen, C., Steffens-Nakken, H., 1995. A novel assay for apoptosis flow cytometric detection of phosphatidylserine early apoptotic cells using fluorescein labelled expression on Annexin V. Phys. B Condens. Matter 184, 39–51. https://doi.org/10.1016/j.physb.2005.01.398.

Clapham, D.E., 1995. Calcium signaling. Cell 80, 259–268. https://doi.org/10.1016/0092-8674(95)90408-5.

Clapham, D.E., 2007. Calcium Signaling. Cell 131, 1047–1058. https://doi.org/10.1016/j.cell.2007.11.028.

Clements, J.A., Nimmo, W.S., Grant, I.S., 1982. Bioavailability, pharmacokinetics, and analgesic activity of ketamine in humans. J. Pharm. Sci. 71, 539–542. https://doi.org/10.1002/jps.2600710516.

Cossart, R., Ikegaya, Y., Yuste, R., 2005. Calcium imaging of cortical networks dynamics. Cell Calcium 37, 451–457. https://doi.org/10.1016/j.ceca.2005.01.013.

Crowley, L.C., Scott, A.P., Marfell, B.J., Boughaba, J.A., Chojnowski, G., Waterhouse, N.J., 2016. Measuring cell death by propidium iodide uptake and flow cytometry. Cold Spring Harb. Protoc. (July), 647–652. https://doi.org/10.1101/pdb.prot087163.

Darzynkiewicz, Z., Galkowski, D., Zhao, H., 2008. Analysis of apoptosis by cytometry using TUNEL assay. Methods 44, 250–254. https://doi.org/10.1016/j.ymeth.2007.11.008.

Demirdaş, A., Nazıroğlu, M., Övey, I.S., 2017. Short-term ketamine treatment decreases oxidative stress without influencing TRPM2 and TRPV1 channel gating in the hippocampus and dorsal root ganglion of rats. Cell. Mol. Neurobiol. 37, 133–144. https://doi.org/10.1007/s10571-016-0353-4.

Dingemans, M.M.L., van den Berg, M., Bergman, Å., Westerink, R.H.S., 2009. Calcium-related processes involved in the inhibition of depolarization-evoked calcium increase by hydroxylated PBDEs in PC12 cells. Toxicol. Sci. 114, 302–309. https://doi.org/10.1093/toxsci/kfp310.

D'Orsi, B., Mateyka, J., Prehn, J.H.M., 2017. Control of mitochondrial physiology and cell death by the Bcl-2 family proteins Bax and Bok. Neurochem. Int. 109, 162–170. https://doi.org/10.1016/j.neuint.2017.03.010.

dos Santos Claro, P.A., Inda, C., Armando, N.G., Piazza, V.G., Attorresi, A., Silberstein, S., 2019. Assessing real-time signaling and agonist-induced CRHR1 internalization by optical methods. In: Shukla, A.K. (Ed.), Methods in Cell Biology. Elsevier Inc, pp. 239–257. https://doi.org/10.1016/bs.mcb.2018.08.009.

Eilers, J., Schneggenburger, R., Konnerth, A., 1995. Patch clamp and calcium imaging in brain slices. In: Sakmann, B., Neher, E. (Eds.), Single-channel Recording. Springer, Boston, MA.

Ghosh, A., Greenberg, E.M., 1995. Calcium Signaling in Neurons: Molecular Mechanisms and Cellular Consequences. 268. pp. 239–247.

Glasgow, N.G., Povysheva, N.V., Azofeifa, A.M., Johnson, J.W., 2017. Memantine and ketamine differentially alter NMDA receptor desensitization. J. Neurosci. 37, 9686 LP–9704. https://doi.org/10.1523/JNEUROSCI.1173-17.2017.

He, Y., Zou, Q., Li, B., Chen, H., Du, X., Weng, S., Luo, T., Zeng, X., 2016. Ketamine inhibits human sperm function by Ca2+ −related mechanism. Biochem. Biophys. Res. Commun. 478 (1), 501–506. https://doi.org/10.1016/j.bbrc.2016.04.144.

Huang, L., Liu, Y., Zhang, P., Kang, R., Liu, Y., Li, X., Bo, L., Dong, Z., 2013. In vitro dose-dependent inhibition of the intracellular spontaneous calcium oscillations in developing hippocampal neurons by ketamine. PLoS One 8, 1–8. https://doi.org/10.1371/journal.pone.0059804.

Ibla, J.C., Hayashi, H., Bajic, D., Soriano, S.G., 2009. Prolonged exposure to ketamine increases brain derived neurotrophic factor levels in developing rat brains. Curr. Drug Saf. 4, 11–16. https://doi.org/10.2174/157488609787354495.

Kress, H.G., Müller, J., Eisert, A., Gilge, U., Tas, P.W., Koschel, K., 1991. Effects of volatile anesthetics on cytoplasmic Ca2+ signaling and transmitter release in a neural cell line. Anesthesiology 74, 309–319.

Krieger, C., Duchen, M.R., 2002. Mitochondria, Ca^{2+} and neurodegenerative disease. Eur. J. Pharmacol. 447, 177–188.

Lalonde, B.R., Wallage, H.R., 2004. Postmortem blood ketamine distribution in two fatalities. J. Anal. Toxicol. 28, 71–74. https://doi.org/10.1093/jat/28.1.71.

Liu, F., Patterson, T.A., Sadovova, N., Zhang, X., Liu, S., Zou, X., Hanig, J.P., Paule, M.G., Slikker, W., Wang, C., 2012. Ketamine-induced neuronal damage and altered N-methyl-d-aspartate receptor function in rat primary forebrain culture. Toxicol. Sci. 131, 548–557. https://doi.org/10.1093/toxsci/kfs296.

McMillin, J.B., Dowhan, W., 2002. Cardiolipin and apoptosis. Biochim. Biophys. Acta 1585, 97–107. https://doi.org/10.1016/S1388-1981(02)00329-3.

Nicotera, P., Orrenius, S., 1998. The role of calcium in apoptosis. BioMetals 11, 375–382. https://doi.org/10.1023/A:1009226316146.

Nutt, L.K., Pataer, A., Pahler, J., Fang, B., Roth, J., McConkey, D.J., Swisher, S.G., 2002. Bax and Bak promote apoptosis by modulating endoplasmic reticular and mitochondrial Ca^{2+} stores. J. Biol. Chem. 277, 9219–9225. https://doi.org/10.1074/jbc.M106817200.

Petit, J.-M., Huet, O., Gallet, P.F., Maftah, A., Ratinaud, M.-H., Julien, R., 1994. Direct analysis and significance of cardiolipin transverse distribution in mitochondrial inner membranes. Eur. J. Biochem. 220, 871–879. https://doi.org/10.1111/j.1432-1033.1994.tb18690.x.

Reutelingspergerg, C.P.M., 1990. Binding of Vascular Anticoagulant α (VACα) to Planar Phospholipid Bilayers. 265. pp. 4923–4928.

Sattler, R., Tymianski, M., 2001. Molecular mechanisms of glutamate receptor-mediated excitotoxic neuronal cell death. Mol. Neurobiol. 24, 107–129. https://doi.org/10.1385/MN:24:1-3:107.

Scorrano, L., Oakes, S.A., Opferman, J.T., Cheng, E.H., Sorcinelli, M.D., Pozzan, T., Korsmeyer, S.J., 2003. BAX and BAK regulation of endoplasmic reticulum Ca2+: a control point for apoptosis. Science 300, 135–139. https://doi.org/10.1126/science.1081208.

Tait, J.F., Gibson, D., Fujikawa, K., 1989. Phospholipid binding properties of human placental anticoagulant protein-I, a member of the lipocortin family. J. Biol. Chem. 264, 7944–7949.

van Loo, G., Saelens, X., van Gurp, M., MacFarlane, M., Martin, S.J., Vandenabeele, P., 2002. The role of mitochondrial factors in apoptosis: a Russian roulette with more than one bullet. Cell Death Differ. 9, 1031.

Wang, C., Zhang, X., Liu, F., Paule, M.G., Slikker, W., 2010. Anesthetic-induced oxidative stress and potential protection. Sci. World J. 10, 1473–1482. https://doi.org/10.1100/tsw.2010.118.

Wang, Y., Tian, K., He, C., Ma, X., Zhang, F., Wang, H., An, D., Heng, B., Jiang, Y., Liu, Y., 2017. Genistein inhibits hypoxia, ischemic-induced death, and apoptosis in PC12 cells. Environ. Toxicol. Pharmacol. 50, 227–233. https://doi.org/10.1016/j.etap.2017.01.022.

Westerink, R.H.S., Ewing, A.G., 2008. The PC12 cell as model for neurosecretion. Acta Physiol. (Oxf.) 192, 273–285. https://doi.org/10.1111/j.1748-1716.2007.01805.x.

Wong, B.S., Martin, C.D., 1993. Ketamine inhibition of cytoplasmic calcium signalling in rat pheochromocytoma (PC-12) cells. Life Sci. 53, 359–364. https://doi.org/10.1016/0024-3205(93)90210-T.

Wood, D., Cottrell, A., Baker, S.C., Southgate, J., Harris, M., Fulford, S., Woodhouse, C., Gillatt, D., 2011. Recreational ketamine: from pleasure to pain. BJU Int. 107, 1881–1884. https://doi.org/10.1111/j.1464-410X.2010.10031.x.

Yamakage, M., Namiki, A., 2002. Calcium channels - basic aspects of their structure, function and gene encoding; anesthetic action on the channels - a review. Can. J. Anesth. 49, 151–164. https://doi.org/10.1007/BF03020488.

Zhivotovsky, B., Orrenius, S., 2011. Calcium and cell death mechanisms: A perspective from the cell death community. Cell Calc. 50, 211–221. https://doi.org/10.1016/j.ceca.2011.03.003.

Zhu, G., Liu, Y., Zhi, Y., Jin, Y., Li, J., Shi, W., Liu, Y., Han, Y., Yu, S., Jiang, J., Zhao, X., 2019. PKA- and Ca 2+ −dependent p38 MAPK/CREB activation protects against manganese-mediated neuronal apoptosis. Toxicol. Lett. 309, 10–19. https://doi.org/10.1016/j.toxlet.2019.04.004.